

We are IntechOpen, the world's leading publisher of Open Access books Built by scientists, for scientists

4,800

Open access books available

122,000

International authors and editors

135M

Downloads

Our authors are among the

154

Countries delivered to

TOP 1%

most cited scientists

12.2%

Contributors from top 500 universities



WEB OF SCIENCE™

Selection of our books indexed in the Book Citation Index
in Web of Science™ Core Collection (BKCI)

Interested in publishing with us?
Contact book.department@intechopen.com

Numbers displayed above are based on latest data collected.
For more information visit www.intechopen.com



Three-Dimensional Digital Colour Camera

Yung-Sheng Chen¹, I-Cheng Chang²,
Bor-Tow Chen³ and Ching-Long Huang³

¹*Department of Electrical Engineering, Yuan Ze University, Chungli,*

²*Department of Computer Science and Information Engineering
National Dong Hwa University, Hualien,*

³*Opto Electronics & Systems Laboratories,
Industrial Technology Research Institute, Hsinchu,
Taiwan, ROC*

1. Introduction

Digital colour camera now has been a popular consumer equipment, has widely used in our daily life, and is highly suited for the next generation of cellular phones, personal digital assistants and other portable communication devices. The main applications of digital colour camera are used to take a digital picture for personal use, picture editing and desktop publishing, high-quality printing, and image processing for advanced academic research. The digital picture is a two-dimensional (2D) form with three-colour components (Red, Green, Blue). The most of efforts for a digital camera producer are focusing on the improvements of image compression, image quality, image resolution, and optical/ digital zooming. However, consider the wide field of computer vision, the depth for a captured object may be another very useful and helpful information, such as surface measurement, virtual reality, object modelling and animation, it will be valuable if the depth information can be obtained while a picture is being captured. In other words, three-dimensional (3D) imaging devices promise to open a very wide variety of applications, particularly, those involving a need to know the precise 3D shape of the human body, e.g. e-commerce (clothing), medicine (assessment, diagnosis), anthropometry (vehicle design), post-production (virtual actors) and industrial design (workspace design) (Siebert & Marshall, 2000). To achieve this significant function, a novel 3-D digital colour camera has been successfully developed by Industrial Technology Research Institute, Opto Electronics & Systems Laboratories (ITRI-OES), in Taiwan. In this article, the previous works, algorithms, structure of our 3D digital colour camera, and 3D results, will be briefly presented.

To obtain 3D information of a given object, the approach may be considered in between a passive scheme and an active scheme. The widely known passive scheme is stereovision, which is useful to measure surfaces with well-defined boundary edges and vertexes. An algorithm to recognize singular points may be used to solve the problem of correspondence between points on both image planes. However the traditional stereoscopic system becomes rather inefficient to measure continuous surfaces, where there are not many reference points. It has also several problems in textural surfaces or in surfaces with lots of discontinuities. Under such an environment, the abundance of reference points can produce

Source: Image Processing, Book edited by: Yung-Sheng Chen,
ISBN 978-953-307-026-1, pp. 572, December 2009, INTECH, Croatia, downloaded from SCIYO.COM

matching mistakes. Thus, an active system based on a structured light concept will be useful (Siebert & Marshall, 2000; Rocchini et al., 2001; Chen & Chen, 2003). In our 3D camera system, the constraint that codifies the pattern projected on the surface has been simplified by using a random speckle pattern, the correspondence problem can be solved by a local spatial-distance computation scheme (Chen & Chen, 2003) or a so-called compressed image correlation algorithm (Hart, 1998).

In our original design, the 3D camera system includes a stereoscopic dual-camera setup, a speckle generator, and a computer capable of high-speed computation. Figure 1(a) shows the first version of our 3D camera system including two CCD cameras needing a distance of 10 cm between its 2 lenses, and a video projector, where the used random speckle pattern in Fig. 1(b) is sent from the computer and projected via the video projector on the measuring object. Each of two cameras takes the snapshot from its own viewpoint, and can do the simultaneous colour image capturing. A local spatial-distance computation scheme or a compressed image correlation (CIC) algorithm then finds some specific speckles on the two camera images. Each of the selected speckles would have its position shown twice, one on each image. After establishing the statistic correlation of the corresponding vectors on the two images, the 3D coordinates of the spots on the object surface will be known from the 3D triangulation.

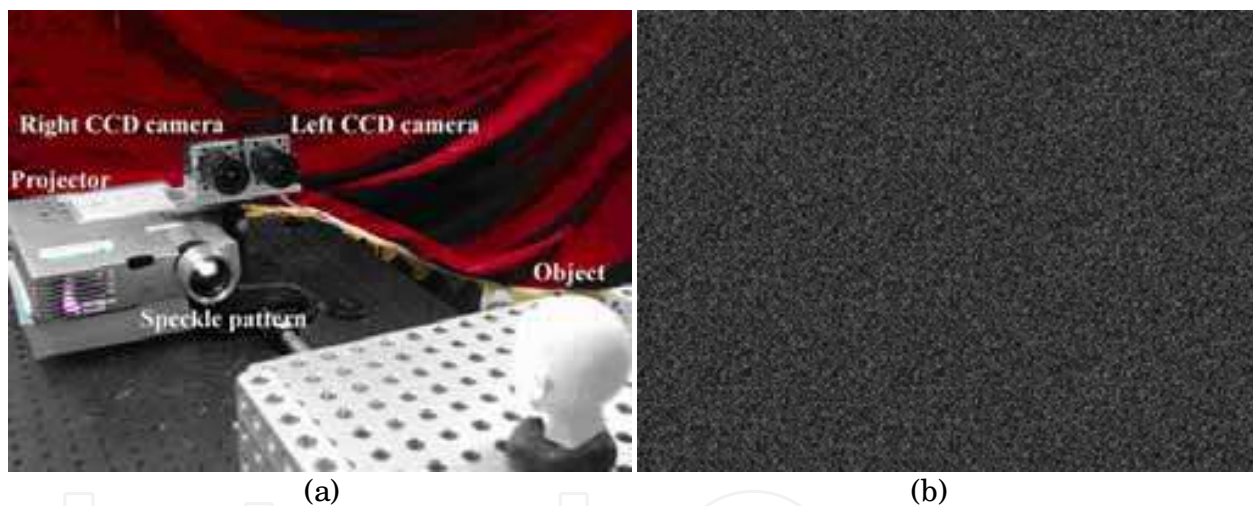


Fig. 1. (a) Our original 3D measurement system. (b) The used random speckle pattern, which is sent from the computer and projected via the video projector.

Not only the traditional stereoscopic systems (Siebert & Marshall, 2000; Rocchini et al., 2001) but also the above mentioned system (Chen & Chen, 2003) are all not easy to be used friendly and popularly due to large system scale, complicated operations, and expensiveness. Hence, to achieve the valuable features (portable, easy operation, inexpensiveness) as possessed by a 2D digital camera, we present a novel design which can be applied to a commercial digital still camera (DSC), and make the 2D camera be able to capture 3D information (Chang et al., 2002). The proposed 3D hand-held camera (the second version of our 3D measurement system) contains three main components: a commercial DSC (Nikon D1 camera body), a patented three-hole aperture lens (Huang, 2001; Chen & Huang, 2002), and a flash. The flash projects the speckle pattern onto the object and the camera captures a single snapshot at the same time. Accordingly, our 3-D hand-held camera

design integrating together the speckle generating projector and the colour digital camera makes the system be able to move around freely when taking pictures.

The rest of this article is organized as follows. Section 2 reviews briefly our previous works. Section 3 presents algorithms for improving 3D measurements. The structure of our novel 3D camera is described in Section 4. Finally a conclusion is given in Section 5. Because the found 3D information should be visualized for the use, all the 3D results are currently manipulated and displayed by our TriD system (TriD, 2002), which is a powerful and versatile modelling tool for 3D captured data, developed by ITRI-OES in Taiwan.

2. Previous works

Our original 3D measurement system shown in Fig. 1(a) includes two CCD cameras and a video projector, where the used random speckle pattern shown in Fig. 1(b) is sent from the computer and projected via the video projector onto the object to be measured. In this system, to solve the correspondence problem of measuring a 3D surface, the random speckle pattern was adopted to simplify the constraint that codifies the pattern projected on the surface and the technique of spatial distance computation was applied to find the correspondence vector (or the correlation vector used in the later of this article).

To effectively perform the correspondence vector finding task, the binarization for the captured image is used in our 3D system developments. The following is our adaptive thresholding method for binarization.

Let a grey block image be defined as G having the size of $m \times m$. The correspondence problem is based on the local matching between two binary block images. Therefore it is important to determine the thresholding value TH , for obtaining the binary block image B . To overcome the uneven-brightness and out-of-focus problem arising from the lighting environment and different CCD cameras, the brightness equalization and image binarization are used. Let m^2 be the total number of pixels of a block image, and $cdf(z)$, $z = 0 \sim 255$ (the grey value index, where each pixel is quantized to a 8-bit data) be the cumulative distribution function of G , then a thresholding controlled by the percentile $p = 0 \sim 100\%$ is defined

$$TH_p = \{z_p \mid cdf(z_p) \approx pm^2\} \quad (1)$$

Thus for a percentile p each grey block image G will have a thresholding value TH_p to obtain its corresponding binary block image B , and we have

$$B(x, y) = \begin{cases} 1 & \text{if } g(x, y) \geq TH_p \\ 0 & \text{otherwise} \end{cases} \quad (2)$$

where 1 and 0 denote the nonzero (white) pixel and the zero (black) pixel, respectively. Note here that the higher the p is, the smaller the data amount having nonzero pixels.

In our previous work, our distance computation approach for finding correspondence vectors is simply described as follows. Let B'_{x_0, y_0} , $x_0 = 0, s, 2s, \dots$; and $y_0 = 0, s, 2s, \dots$, be a binary block image in the left-captured image starting at the location (x_0, y_0) , where s is the sampling interval from the captured image. The searched block image, B'_{u_0, v_0} starting at the location (u_0, v_0) in the right-captured image, will be in the range of u_0 in $[x_0 - R_x, x_0 + R_x]$ and

v_0 in $[y_0 - R_y, y_0 + R_y]$, where R_x and R_y depend on the system configuration. If the CCD configuration satisfies to the epipolar line constraint, then R_y can be very small. In the searching range, if a right binary block image B_{u_f, v_f}^r has the minimum spatial distance $d(B_{x_0, y_0}^l, B_{u_f, v_f}^r)$ between it to B_{x_0, y_0}^l , then the vector from (x_0, y_0) to (u_f, v_f) is defined to be the found correspondence vector.

Because the corresponding information used in the stereoscopic system are usually represented with the subpixel level, in this version of 3D system, a simple averaging with an area A of size $w \times w$ containing the found correspondence results (u_f, v_f) s is used to obtain the desired subpixel coordinate (u_f^*, v_f^*) and is expressed by

$$u_f^* = \frac{1}{N} \sum_{\forall (u_f, v_f) \in A} u_f \quad \text{and} \quad v_f^* = \frac{1}{N} \sum_{\forall (u_f, v_f) \in A} v_f \quad (3)$$

The more details of measuring a 3D surface using this distance computation scheme can be found in the literature (Chen & Chen, 2003). A result is given in Fig. 2 for illustration, where (a) and (b) show the captured left and right images; (c) displays the reconstructed 3D surface along some manipulations performed on the TriD system (TriD, 2000).

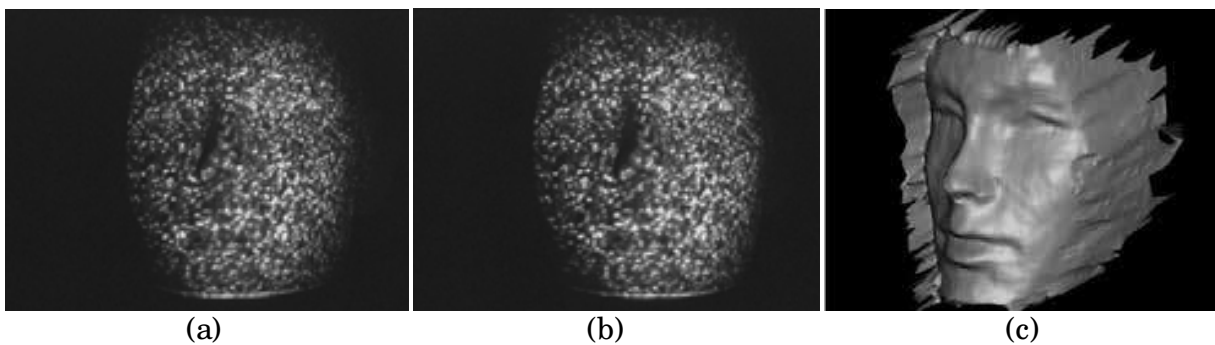


Fig. 2. (a) Left captured image, and (b) right captured image for the object shown in Fig. 1(a). The image size is 640×480 . (c) The reconstructed 3D surface with the method presented in (Chen & Chen, 2003), where $p = 65\%$, $s = 4$, and a 5×5 support for subpixel compensation were used.

3. Algorithms for improving 3D measurement

In order to investigate the accuracy of 3D information, we have developed another approach different to our previous spatial distance computation for improving our system. This idea comes from the analysis of partial image velocimetry using compressed image correlation (Hart, 1998). In the following, under a hierarchical search scheme, pixel level computation and subpixel level computation combined with brightness compensation will be presented for approaching to the goal of improving 3D measurement.

3.1 Pixel level computation

A hierarchical search scheme is adopted in pixel level computation. First let the left image be divided into a set of larger fixed-size blocks, and called level 1 the top layer. Consider a block B_1^l in left image, if one block B_1^r in right image has the best correlation then the vector

V_1 from the coordinate of B_1^l to that of B_1^r is found. Based on the facility of coarse-to-fine, the next search is confined to the range indicated by V_1 in right image and the execution time can be further reduced. Hence next, let the block image B_1^l in level 1 be further divided into four subblocks, this is the level 2. Consider the subblock B_2^l in B_1^l having the same coordinate, by the vector V_1 , the correlation process is further performed only on the neighboring subblocks centered at the coordinate of B_1^r . The best correlation conducting the vector V_2 from the coordinate of B_2^l to one subblock B_2^r is found. Continue this process, if the best match is found and ended at level n , then the final vector of best correlation may be expressed as

$$V = \sum_{i=1}^n V_i \quad (4)$$

In order to reduce the computation time of correlation, a so-called correlation error function for an $M \times N$ image is used and defined as follows (Hart, 1998).

$$\phi_{\Delta i, \Delta j} = \frac{\sum_{m=1}^M \sum_{n=1}^N (I_{m,n} + I_{m+\Delta i, n+\Delta j} - |I_{m,n} - I_{m+\Delta i, n+\Delta j}|)}{\sum_{m=1}^M \sum_{n=1}^N (I_{m,n} + I_{m+\Delta i, n+\Delta j})} \quad (5)$$

This function only uses addition and subtraction, thus the time reduction is expectable. Note here that the processed images I s are binarized after adaptive thresholding as described in Section 2, thus the information of I s are only either 1 or 0.

3.2 Subpixel level computation

In order to increase the accuracy of the correspondence finding, two schemes are combined for achieving this purpose. One is grey scale interpolation, the other is brightness compensation. For grey scale interpolation, a linear scheme is performed on the third layer of right image. In our study, the block size of the third layer is 8×8 . The processing includes two steps as follows.

Step 1. Use the pixel grey levels in vertical direction to interpolate the subpixel grey level, e.g., 3-point interpolation, between two neighboring pixels.

Step 2. Based on the pixel and subpixel grey levels found in Step 1 to interpolate the subpixel grey levels in horizontal direction. In this case, the 3-point interpolation is also considered as example.

A comparison among pixel level, subpixel level, and after interpolation is illustrated in Fig. 3(a)-(c), respectively. Here we observe the image in Fig. 3(c) that the smoothness is improved greatly within the middle image but the randomness becomes more serious at two sides. It results from the ununiform brightness between the two CCD cameras. Hence a brightness compensation scheme is presented to solve this problem.

As mentioned before for correlation error function in (5), the used correlation function (CF) may be redefined as

$$CF = \frac{I_1 + I_2 - |I_1 - I_2|}{I_1 + I_2}, \quad (6)$$

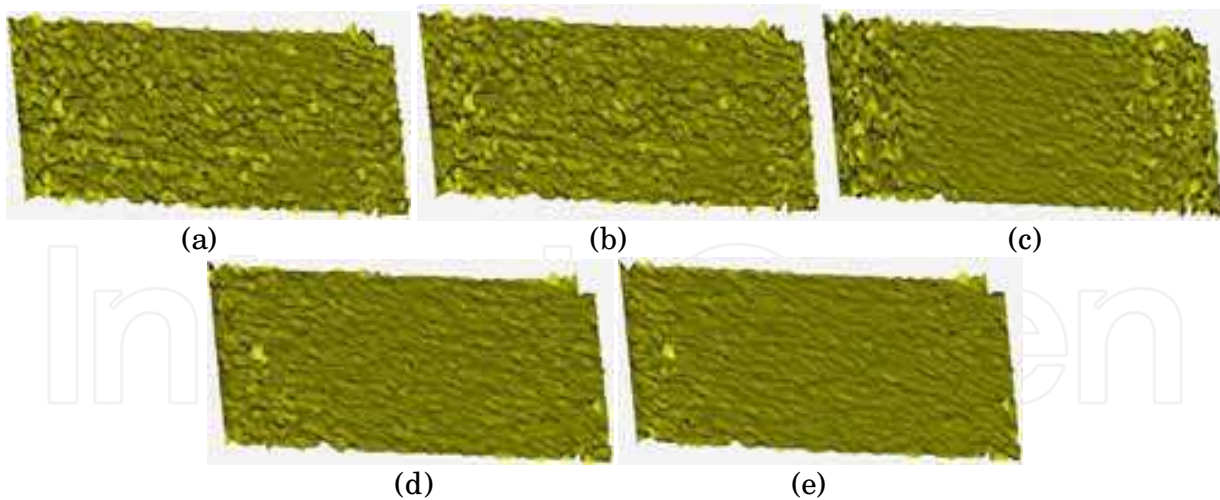


Fig. 3. Correlation results of (a) pixel level, (b) subpixel level, and (c) after interpolation. Further improved results using interpolation with (d) BC 32, and (e) BC 64.

where

$$CF = \begin{cases} \frac{2I_2}{I_1 + I_2} & \text{if } I_1 \geq I_2, \\ \frac{2I_1}{I_1 + I_2} & \text{otherwise.} \end{cases} \quad (7)$$

Consider (7), if two block images I_1 and I_2 have different brightness, the correlation from I_1 to I_2 will be different to that from I_2 to I_1 . Furthermore, it will be dominated by the block image having lower grey level distribution. As a result, the more uniform the two block image distribution, the higher accuracy the correlation; and vice versa. To compensate such ununiform brightness between two block images and reduce the error, a local compensation factor (LCF) is introduced as

$$LCF = \frac{\sum_{(x_i, y_i) \in \text{left block}} P(x_i, y_i)}{\sum_{(x_j, y_j) \in \text{right block}} P(x_j, y_j)}, \quad (8)$$

thus now (6) is modified as below and named CF with brightness compensation (BC).

$$CF_{BC} = \frac{I_1 + LCF \times I_2 - |I_1 - LCF \times I_2|}{I_1 + LCF \times I_2} \quad (9)$$

According to (9), results in Fig. 3(d) and 3(e) show that a good quality can be obtained. Here BC 32 means that 32 feature points are used in the subcorrelation. In our experiments, the accuracy can be increased 0.2-0.3 mm by the scheme of interpolation with brightness compensation; however a trade-off is that 4-5 times of computational time will be spent.

3.3 Results

Consider the two captured images shown in Fig. 2(a) and 2(b) respectively, three reconstructed results using pixel level computation, subpixel level computation, and the

further improvement by interpolation with BC are shown in Fig. 4(a), 4(b), and 4(c), respectively. Obviously, the later result shows a better performance.

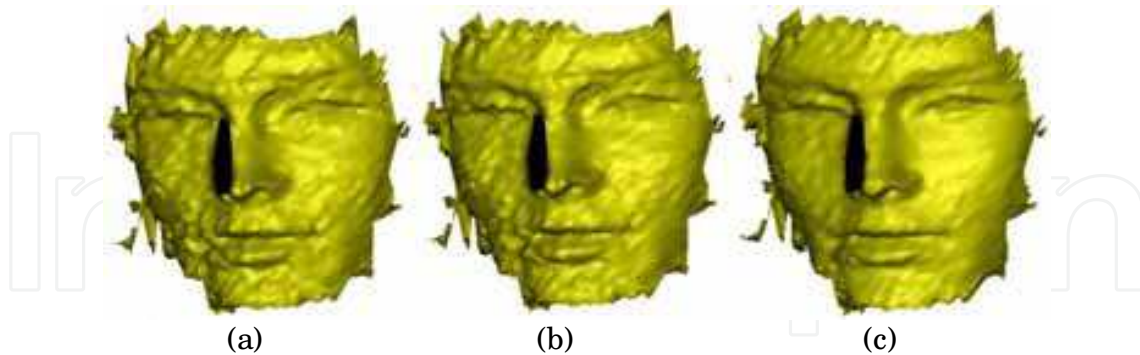


Fig. 4. Reconstructed results using (a) pixel level computation, (b) subpixel level computation, and (c) the further improvement by interpolation with BC.

In order to further increase the accuracy of reconstructing 3D object, a suitable method is to use a high resolution CCD system for capturing more data for an object. For example, in our system, Fig. 5(a) shows a normal resolution result with 652×512 , whereas Fig. 5(b) shows a high resolution result with 1304×1024 . Their specifications are listed in Table 1.

For a high resolution CCD system, due to more data to be processed we present a simplified procedure to solve the time-consuming problem. Consider the case of 1304×1024 , the processing procedure is as follows.

Step 1. Down sampling. The image is reduced to a 652×512 resolution.

Step 2. Pixel level correlation with 3 levels is performed on the 652×512 image. In this step, the coarse 80×64 correlation vectors are obtained at the lowest level.

Step 3. Lift the lowest level in pixel level correlation from 8×8 to 16×16 each block, and further perform the pixel level computation on the original 1304×1024 image. Thus there are 160×128 correlation vectors to be output in this step.

Step 4. Based on the correlation vectors obtained in steps 3 and 4, the subpixel level correlation is performed to produce the final results.

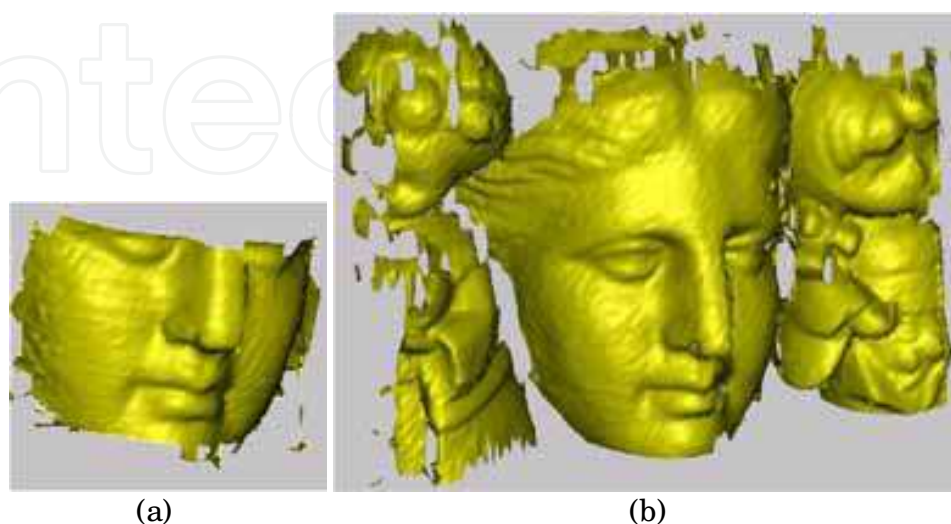


Fig. 5. Examples of (a) normal resolution, and (b) high resolution.

System specification	Normal resolution system	High resolution system
Baseline (mm)	70	100
Lens (mm)	600	700
Object-CCD Distance (mm)	35	28
View Range (mm×mm)	83×62^a	180×150
Image Density Resolution	7.7×7.7^b	7.2×6.8

^a “View Range” is defined as the (object width) × (object height).

^b “Image Density Resolution” is defined as (image width/ object width) × (image height/ object height), thus the unit is (pixel/ mm) × (pixel/ mm).

Table 1. Comparison between a normal and a high resolution CCD system in our study.

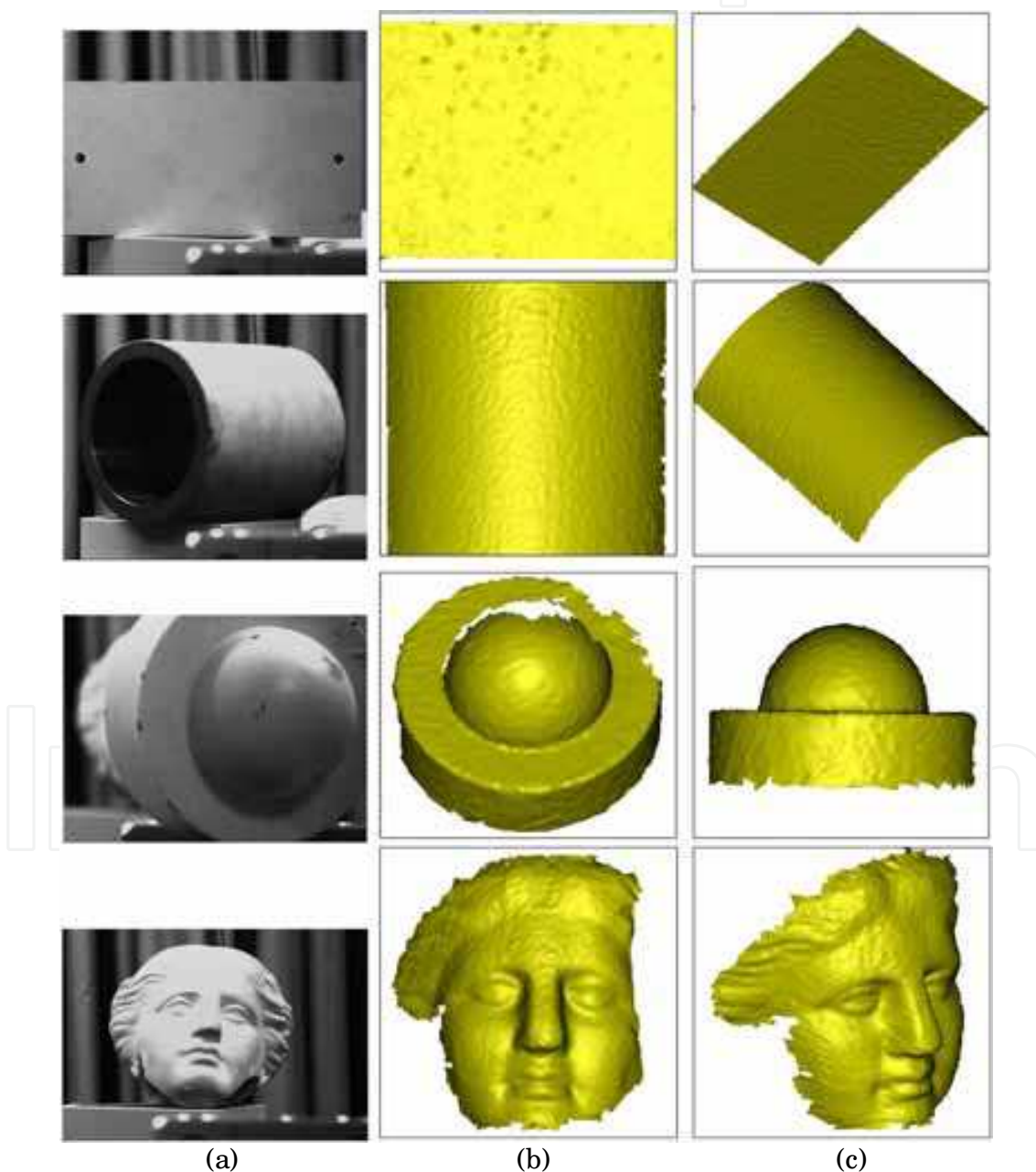


Fig. 6. Four test objects in (a), and their results with different views in (b) and (c).

For further demonstrating the quality of our algorithms, four objects in Fig. 6(a) and their reconstructed results in Fig. 6(b) and 6(c) are given. Note here that these results are only obtained from one view, thus they can be regarded as a 2.5D range image data. If multiple views are adopted and manipulated by our TriD system, the totally 3D result can be generated and illustrated in Fig. 7. As a result, a set of effective algorithms have been successfully developed for our 3D measurement system.

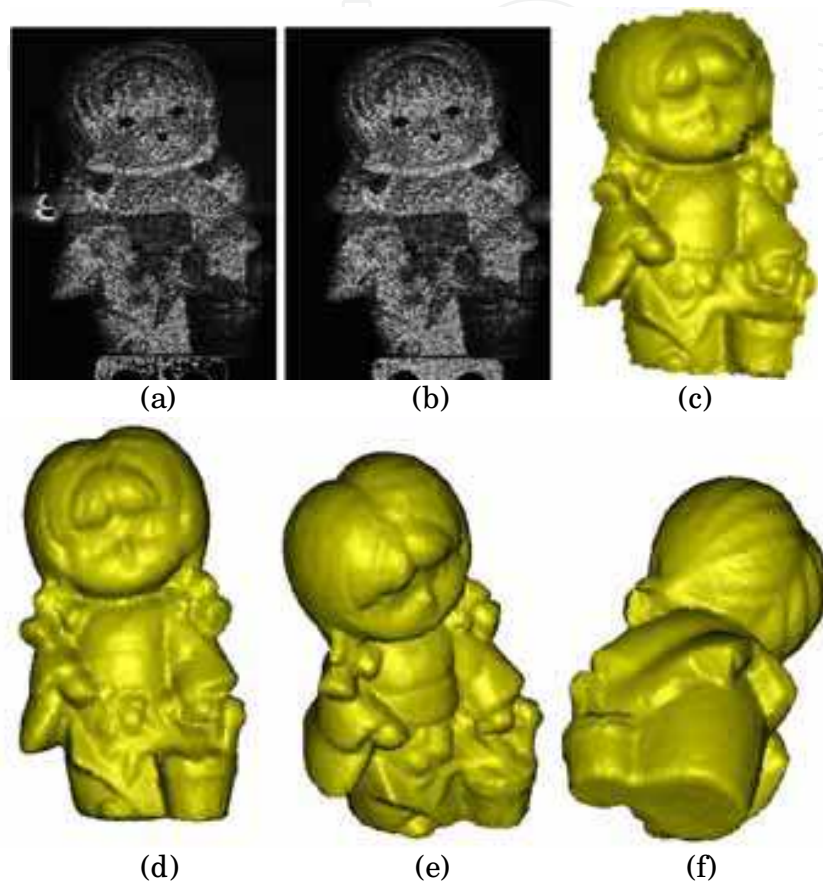


Fig. 7. Reconstructed 3D result of a doll. (a)(b) Speckled images. (c) 2.5D range image data using the speckled images. (d)-(f) Complete 3D result using many 2.5D range data.

4. 3-D Camera

The proposed 3D hand-held camera contains three main components: a commercial DSC (Nikon D1 camera body), a patented three-hole aperture lens (Huang, 2001; Chen & Huang, 2002), and a flash as shown in Fig. 8(a). The flash projects the speckle pattern onto the object and the camera captures a single snapshot at the same time. To embed the 3D information in one captured image, we devise a novel lens containing three off-axis apertures, where each aperture was attached one colour filter as depicted in Fig. 8(b), so that a captured image carries the information from three different viewing directions. Since the three different images can be extracted from filtering the captured image with red, green, and blue component, respectively, the depth information may be obtained from these images by using the algorithms introduced in Section 3.

For the sake of illustrating the principle of our tri-aperture structure, an example of lens with two apertures is depicted in Fig. 8(c). Three points, P1, P2, and P3 are set on the central

axis, where P_2 is located at focal plane; P_1 and P_3 located at a far and near points with respect to the lens. The rays reflected from P_2 pass through aperture A and B will intersect at the same location on the image plane, whereas P_1 or P_3 will image two different points. Accordingly the depth information of P_1 and P_3 may be computed from the disparity of their corresponding points on the image plane.

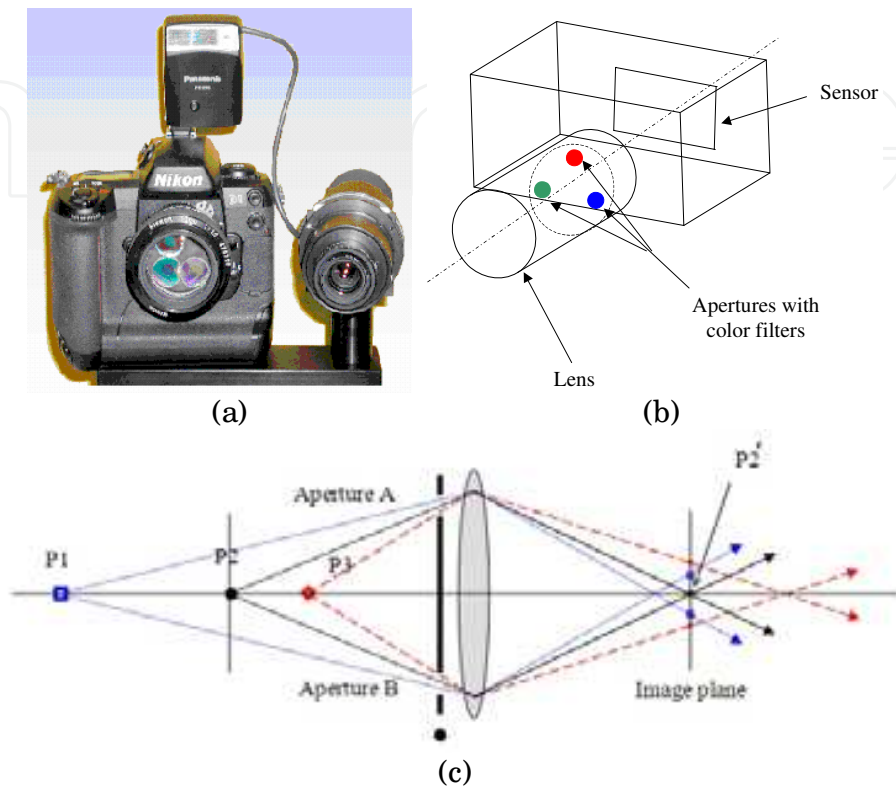


Fig. 8. (a) The newly designed version is based on a commercial digital camera (Nikon D1 camera body), a patented ring-aperture (three-hole aperture) lens depicted in (b), and a flash projecting a speckle pattern. (c) Example of lens with two apertures.

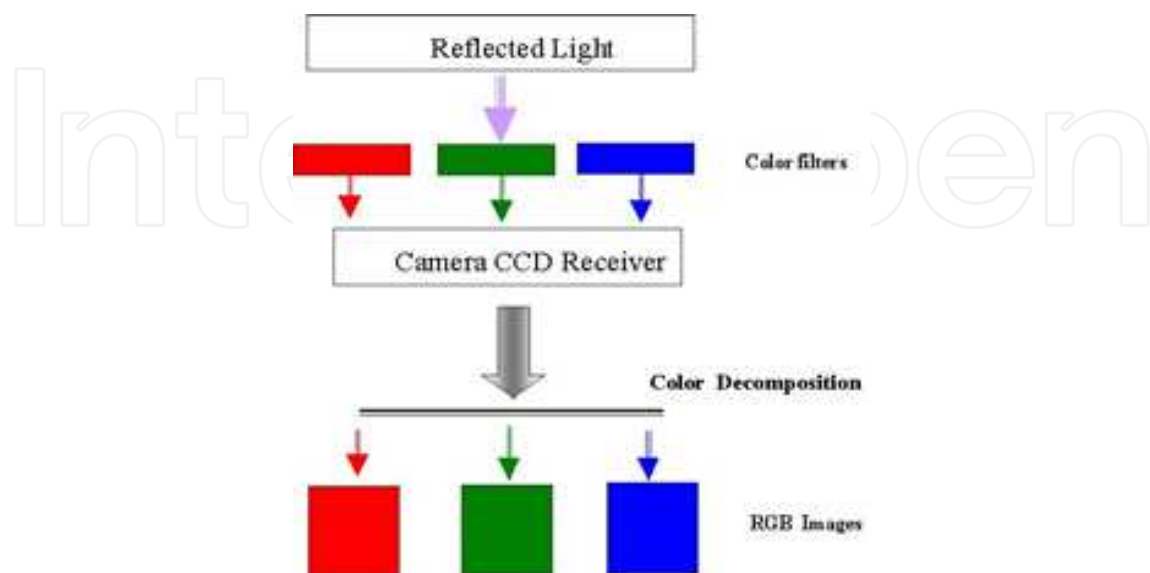


Fig. 9. Colour composition and decomposition

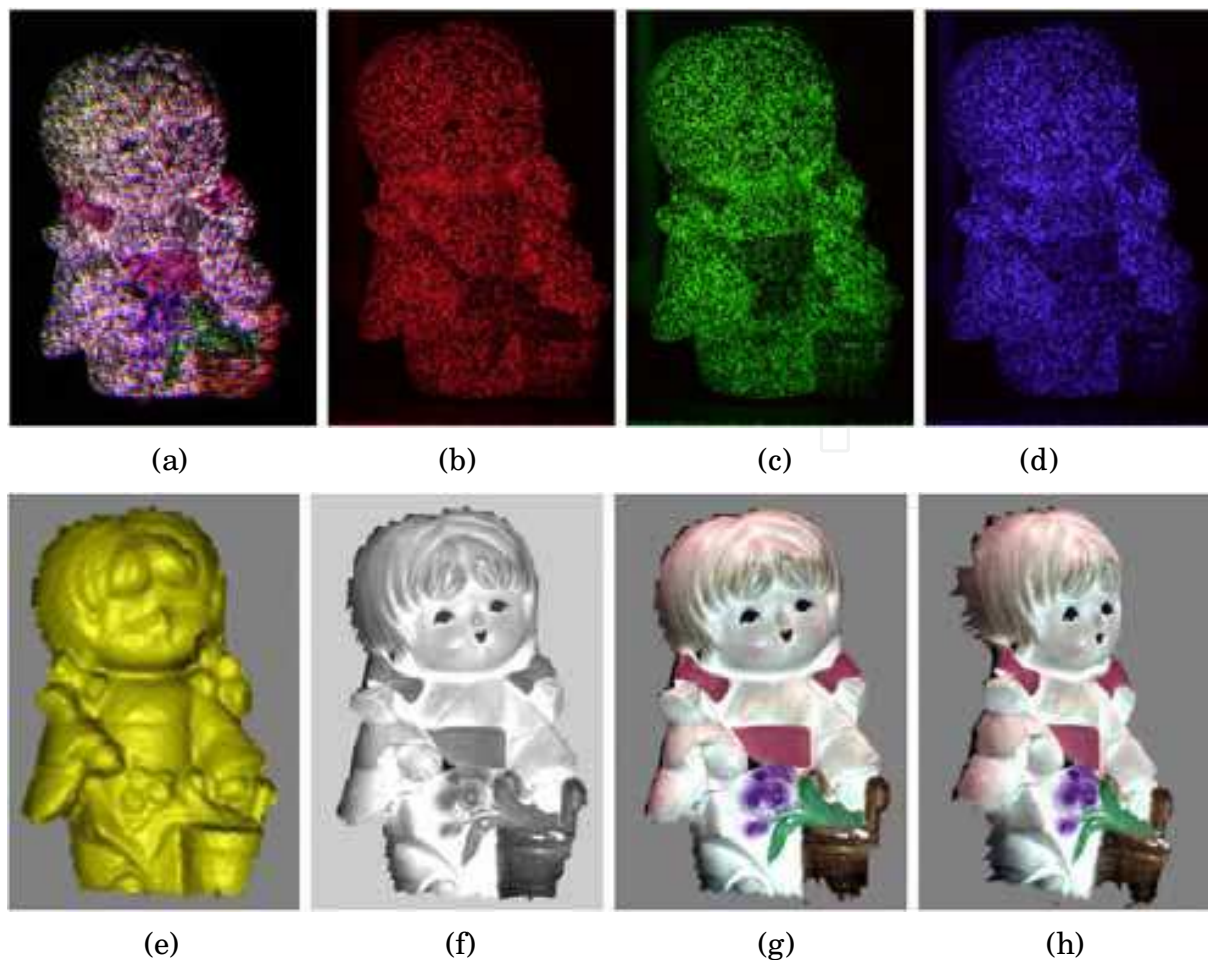


Fig. 10. (a) Image from tri-aperture lens. (b)-(d) R, G and B component obtained by separating the image from tri-aperture lens. (e) Range data. (f) Grey textured 2.5D image. (g)-(h) Colour textured 2.5D image with different view angles.

To extract the depth information from the single image, the image should be separated based on the colour filter. The colour composition and decomposition in Fig. 9 and an example shown in Fig. 10 are given for illustration. In Fig. 10(a), the image shows a mixture of R, G, B colour pixels since it merges the images from different direction and colour filters. After colour separation process, three distinguished images based on R, G, B components are obtained as shown in Fig. 10(b)-10(d). Based on our depth computation algorithm embedded in TriD system, the range data is obtained as Fig. 10(e) shows. If a grey image is applied, we can obtain a grey textured 2.5D image as Fig. 10(f) using a rendering process in TriD. Similarly, once a colour image is fed into our system, a colour textured 2.5D image may also be obtained as shown in Fig. 10(g) and 10(h) with different view angles. Note here that in this processing, a cross-talk problem may be risen, i.e., G and B components may corrupt the R-filtering image for example. In our study, this problem may be solved by increasing image intensity while an image is being captured.

The processing stages of our acquisition system using the proposed 3D camera are as follows. The camera captures two images of the target. The first snap gets speckled image (for 3D information computation), which will be spilt into three images based on the colour decomposition described before. Then the correlation process is used to compute depth

information. The second snap gets original image (as a texture image) for further model rendering. For example, the human face of one author (Chang, I. C.) of this article is used for modelling. The speckled and texture images are captured and shown in Fig. 11(a) and 11(b), respectively. After the TriD software system, a face 3D model and its mesh model are obtained as shown in Fig. 11(c) and 11(d), respectively. This result demonstrates the feasibility of our 3-D hand-held camera system.

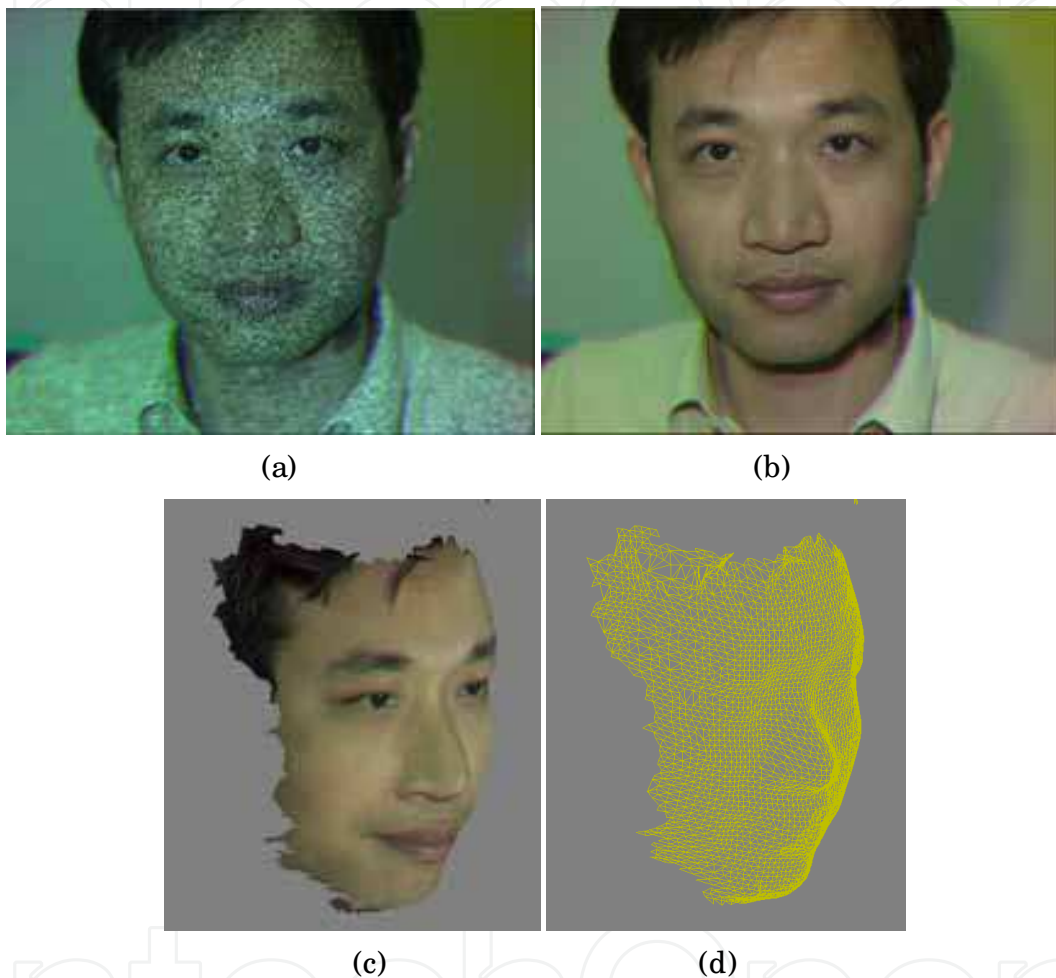


Fig. 11. The speckled image (a) and texture image (b) taken by our 3D hand-held camera system. The 3D face model (c) and its mesh model (d) manipulated by our TriD system.

As described above, using the typical digital camera with our patented three-hole aperture lens along with a high accuracy calculation, the entire 3D image capturing process can now be done directly with a single lens in our 3D camera system. The three-hole aperture provides more 3D information than the dual-camera system because of their multi-view property. The depth resolution can therefore be increased considerably. Currently this 3D camera system has reached precision of sub-millimetre. The main system specifications are listed in Table 2. As a result, our 3D hand-held camera design integrating together the speckle generating projector and the colour digital camera makes the system be able to move around freely when taking pictures.

Light source	(flash) White-light random speckle pattern
CCD resolution	2000×1312
Measuring distance	500 ~ 800 mm
Measuring range	360 mm (X) × 240 mm (Y) × 80 mm (Z)
Resolution	0.18 mm (X) × 0.18 mm (Y)
Image capturing speed	1/ 30 second capturing time and 20 second processing time
Colour	R, G, B each 8 bits
Software	Plug-in module in <i>TriD</i> system

Table 2. System specifications in our 3-D hand-held camera design.

5. Conclusion

Three-dimensional information wanted has been an important topic and interested to many real applications. However, it is not easy to obtain the 3D information due to several inherent constraints on real objects and imaging devices. In this article, based on our study in recent years, we present effective algorithms using random speckle pattern projected on an object to obtain the useful correspondence or correlation vectors and thus reconstruct the 3D information for an object. Original two CCD cameras system has also been moved to a novel 3D hand-held camera containing a DSC, a patented three-hole aperture lens and a flash projecting random speckle pattern. Based on the manipulations of our TriD software system, our experiments have confirmed the feasibility of the proposed algorithms and 3D camera. This result guides us to a new era of portable 3D digital colour camera.

6. References

- Chang, I. C.; Huang, C. L. & Hsueh, W. J. (2002). Novel three-dimensional hand-held camera based on three-aperture lens, *Proceedings of SPIE on Photonics Asia: Electronic Imaging and Multimedia Technology III*, Vol. 4925, pp. 655-662, Shanghai, China, Oct. 15-17, 2002.
- Chen, B. T. & Huang, C. L. (2002). Device and methodology of capturing three-dimensional data using single len, *Patent number 154398*, Taiwan, ROC, 2002-2021.
- Chen, Y. S. & Chen, B. T. (2003). Measuring of a three-dimensional surface by use of a spatial distance computation, *Applied Optics*, Vol. 42, No. 11, pp. 1958-1972.
- Hart, D. P. (1998). High-speed PIV analysis using compressed image correlation, *Journal of Fluids Engineering*, Vol. 120, pp. 463-470.
- Huang, C. L. (2001). Three-dimensional capturing device using single lens, *Patent number 139230*, Taiwan, ROC, 2001-2020.
- Rocchini, C.; Cignoni, P.; Montani, C.; Pingi, P. & Scopigno, R. (2001). A low cost 3D scanner based on structured light, *Computer Graphics Forum, Proceedings of EUROGRAPHICS*, Vol. 20, pp. 299-308.
- Siebert, J. P. & Marshall, S. J. (2000). Human body 3D imaging by speckle texture projection photogrammetry, *Sensor Review*, Vol. 20, pp. 218-226.

(2002). *TriD: Technical Report for 3D Human Modeling & Animation Application*, ver. 2.0, Opto-Electronics & Systems Laboratories, Industrial Technology Research Institute, Taiwan, ROC.

IntechOpen

IntechOpen



Image Processing

Edited by Yung-Sheng Chen

ISBN 978-953-307-026-1

Hard cover, 516 pages

Publisher InTech

Published online 01, December, 2009

Published in print edition December, 2009

There are six sections in this book. The first section presents basic image processing techniques, such as image acquisition, storage, retrieval, transformation, filtering, and parallel computing. Then, some applications, such as road sign recognition, air quality monitoring, remote sensed image analysis, and diagnosis of industrial parts are considered. Subsequently, the application of image processing for the special eye examination and a newly three-dimensional digital camera are introduced. On the other hand, the section of medical imaging will show the applications of nuclear imaging, ultrasound imaging, and biology. The section of neural fuzzy presents the topics of image recognition, self-learning, image restoration, as well as evolutionary. The final section will show how to implement the hardware design based on the SoC or FPGA to accelerate image processing.

How to reference

In order to correctly reference this scholarly work, feel free to copy and paste the following:

Yung-Sheng Chen, I-Cheng Chang, Bor-Tow Chen and Ching-Long Huang (2009). Three-Dimensional Digital Colour Camera, Image Processing, Yung-Sheng Chen (Ed.), ISBN: 978-953-307-026-1, InTech, Available from: <http://www.intechopen.com/books/image-processing/three-dimensional-digital-colour-camera>

INTECH
open science | open minds

InTech Europe

University Campus STeP Ri
Slavka Krautzeka 83/A
51000 Rijeka, Croatia
Phone: +385 (51) 770 447
Fax: +385 (51) 686 166
www.intechopen.com

InTech China

Unit 405, Office Block, Hotel Equatorial Shanghai
No.65, Yan An Road (West), Shanghai, 200040, China
中国上海市延安西路65号上海国际贵都大饭店办公楼405单元
Phone: +86-21-62489820
Fax: +86-21-62489821

© 2009 The Author(s). Licensee IntechOpen. This chapter is distributed under the terms of the [Creative Commons Attribution-NonCommercial-ShareAlike-3.0 License](https://creativecommons.org/licenses/by-nc-sa/3.0/), which permits use, distribution and reproduction for non-commercial purposes, provided the original is properly cited and derivative works building on this content are distributed under the same license.

IntechOpen

IntechOpen